

Strong $M1$ transitions in ^{23}Na below 10 MeV

R. Vodhanel,* M. K. Brussel, R. Moreh,† W. C. Sellyey, and T. E. Chapuran‡
 Department of Physics, University of Illinois at Urbana—Champaign, Urbana, Illinois 61801
 (Received 14 September 1983)

A bremsstrahlung photon beam from electrons with end-point energies of 7.66 and 10.37 MeV was used for photoexciting levels in ^{23}Na . Values of $g\Gamma_0^2/\Gamma$ and $g\Gamma_0$ of 22 levels below 10 MeV were obtained using scattering and self-absorption measurements. The values for 7 levels are reported for the first time. The temperature variation of the scattering cross section was measured at $T=300$ K and $T=78$ K to study in some detail the effective temperature T_e of metallic ^{23}Na . The results of the total $B(M1\uparrow)$ strength of $T=\frac{1}{2}$ levels below 9 MeV were found to be in excellent agreement with the large-scale shell-model calculations.

[NUCLEAR REACTIONS $^{23}\text{Na}(\gamma, \gamma')$, $E=7.66, 10.37$ MeV bremsstrahlung.
 Deduced $E_x, g\Gamma_0, B(M1\uparrow)$. Natural target.]

I. INTRODUCTION

The interest in the ^{23}Na nucleus arises from its being an odd nucleus in the s - d shell region having a relatively large deformation. Thus it constitutes a favorable nucleus for testing the particle-rotor model. In fact, several levels of ^{23}Na have been described as members of rotational bands built upon intrinsic single particle states.¹⁻⁴ It should be noted, however, that the large-scale shell model calculations of McGrory and Wildenthal⁵ seem to reproduce nicely not only the static properties of ^{23}Na , such as its ground state magnetic moment and its electric quadrupole moment, but also the excitation energies and the dynamic properties such as the rates of the electromagnetic transitions between the various levels.

The measurement of the widths of the above levels constitute a most sensitive test of any theoretical model trying to describe the states of ^{23}Na . The ^{23}Na levels are of further interest as they are used for flux calibration purposes in nuclear resonance fluorescence (NRF) experiments with bremsstrahlung.

In the past, the width of the ^{23}Na levels were measured using bremsstrahlung^{6,7} and employing the NRF technique. However, in that work no self-absorption measurements were carried out, and the ground state widths were obtained using calibration levels of known widths in ^{11}B . Some self-absorption data were reported on a few levels below 7.1 MeV in ^{23}Na using either bremsstrahlung photons or quasimonochromatic photons emitted from the $^{19}\text{F}(\alpha, p)^{16}\text{O}$, and the $^{15}\text{N}(p, \alpha)^{12}\text{C}$ reactions.^{8,9}

The use of self-absorption for the determination of level widths is advantageous because the result is independent of the intensity of the incident beam which is a principal source of uncertainty. However, such a measurement requires an accurate knowledge of the Doppler width, $\Delta = \sqrt{2kT_e/Mc^2}$, which depends on the effective temperature T_e . The value of T_e is usually calculated using the Lamb formula^{10,11} but this has been found to produce inconsistent results in the case of ^{11}B and in some molecu-

lar compounds.^{12,13} It was therefore thought to be advisable to test this formula again for ^{23}Na (as was done in the case of ^{11}B). The results indicated that the use of the Lamb formula for calculating T_e was appropriate for the case of *metallic* ^{13}Na .

II. EXPERIMENTAL PROCEDURE

The incident bremsstrahlung was produced using 7.66 and 10.37 MeV electron beams and $\lesssim 15 \mu\text{A}$ currents from our 100% duty cycle MUSL-2 accelerator.¹⁴ These electron beams traversed 76 or 196 mg/cm² gold foil radiators. These are then stopped by a thick graphite block placed in a Faraday cup which monitored the beam intensity. The experimental arrangement is essentially that given in Ref. 15. The only difference was the use of a 5 cm thick borated paraffin shield around our 55 cm³ Ge(Li) detector. The use of this shield was found to be very effective against the fast neutron background. The face of the detector was situated at a scattering angle of 127° with respect to the incident photon beam and at a distance of 35 cm from the target. A photon hardener consisting of copper (6.0 cm), lead (2.15 cm), and borated paraffin (5.0 cm), placed in front of the detector was used. The γ -ray energy resolution of the system was ~ 10 keV FWHM at $E_\gamma=8$ MeV for counting rates of $\sim 3 \times 10^4/\text{sec}$. The electronics and the data acquisition method used are described elsewhere.^{15,16}

Square 10×10 cm² targets of NaOH (4.18 g/cm² of Na) and metallic Na, 3.74 g/cm² thick, placed in 4 mm thick Lucite containers were used for scattering measurements. For self-absorption, *metallic* targets together with *metallic* absorbers having thicknesses of 3.80, 7.46, and 11.26 g/cm² were used. Comparison absorbers of metallic magnesium were employed to account for the atomic attenuation of the bremsstrahlung beam.

In the temperature variation measurements, a 7.46 g/cm² thick metallic Na absorber (situated near the bremsstrahlung source) and a 3.61 g/cm² thick metallic

Na target were used. This target was enclosed in a thin aluminum foil after being immersed in liquid paraffin to avoid oxidation. The scattered intensities at $T=78$ K (liquid nitrogen temperature) and $T=300$ K were compared. The reason for employing a resonant absorber in this measurement will be explained in Sec. III E.

III. RESULTS AND DATA ANALYSIS

A. Scattered spectra

Figure 1 shows the measured spectrum of photons scattered from the Na target (using 10.37 MeV bremsstrahlung). This spectrum is the sum of six resonant and non-resonant absorption spectra and is given here because of its high statistics; it enables accurate branching ratio determinations for several levels. Table I lists the identified transitions of this spectrum. In addition, it shows a few "background" lines at 6917 and 7117 keV which are owing to elastic scattering from ^{16}O present in the Lucite container of the target. The 2223 keV γ line of the $^1\text{H}(n,\gamma)^2\text{H}$ was also observed. The 4439 γ line owing to the scattering from the first excited state of ^{12}C was obscured by the very intense 4432 keV γ line of ^{23}Na . The excitation energies of the ^{23}Na levels (Table I) were deduced from the spectra after correcting for nuclear recoil. The results are generally consistent with the values adopted by Endt and Van der Leun.¹⁷

B. Branching ratios

The branching ratio, Γ_i/Γ , of each level was determined by measuring the relative intensities at $\theta=127^\circ$ of the observed inelastic branches to low-lying excited states. Corrections were made for the energy dependence of the detector efficiency. It was assumed that the angular distribution of the scattered radiation is $W(\theta)=1+A_2P_2(\cos\theta)$. This implies that either pure dipole or mixed dipole-quadrupole transitions are involved. The results of Γ_i/Γ for some levels in ^{23}Na are listed in Table II. This table also gives our adopted values of the ground state branching ratio Γ_0/Γ based on comparisons of the present and previous results.¹⁷

C. Scattering cross sections

Values of $g\Gamma_0^2/\Gamma$ of the ^{23}Na levels were obtained from a knowledge of the flux-efficiency product $N_\gamma(E)\epsilon(E)$ for $E \gtrsim 3$ MeV. This product was determined for electron beam energies $E_e=7.66$ and 10.37 MeV and for the two thicknesses of the Au radiator by measuring the scattering intensities from calibration levels in ^{11}B , ^{24}Mg , ^{27}Al , ^{31}P , ^{88}Sr , and ^{208}Pb whose widths are accurately known.^{12,15,17,18} These results were combined with values of Γ_0/Γ to determine $g\Gamma_0^2/\Gamma$ and hence the scattering cross sections. A curve was drawn through the experimental points of $N_\gamma(E)\epsilon(E)$ vs E using a least squares procedure with quadratic and cubic functions of E . More details about this procedure¹⁵ may be found elsewhere. This curve together with the scattering intensities from the ^{23}Na target was used to deduce the scattering cross

sections and hence the values of $g\Gamma_0^2/\Gamma$ for the ^{23}Na levels. By combining those results with the measured branching ratios Γ_0/Γ , the values of $g\Gamma_0$ were deduced. For some ^{23}Na levels below 7.3 MeV, two separate determinations of $g\Gamma_0^2/\Gamma$ were made corresponding to the two incident energies at $E_e=7.66$ and 10.37 MeV. The results of the two measurements were in good agreement apart from the levels at 2982 and 3915 keV where the 10.37 MeV results were higher by 20% and 50%, respectively. We attribute the discrepancies to the feeding of those levels from higher energy levels. Thus, for those two levels, the 7.66 MeV results were adopted after corrections for feeding from higher levels. The $g\Gamma_0$ for 14 levels in ^{23}Na determined by the above procedure are listed in Table III.

D. Self-absorption

Three sets of self-absorption measurements¹¹ were carried out, corresponding to the different Na-absorber thicknesses, to determine $g\Gamma_0$ of the strongly excited levels at 4432, 5741, 5766, 6735, 7070, 7082, 7890, 8360, 8662 keV. The atomic attenuation of the photons was measured using Mg absorbers having an equivalent "atomic" thickness to those of the Na absorbers. Typically, the nuclear attenuation factors R varied between 0.2 and 0.6, depending on the absorber thickness and the nuclear level parameters. The values of $g\Gamma_0$ were then extracted from the experimental data by using the following procedure: Pairs of values of (Γ_0, Γ) were deduced which yielded the measured value of the nuclear absorption. In doing so, a computer program was used which accounted for the nuclear absorption in the absorber and in the scatterer. These values of (Γ_0, Γ) together with their errors constitute a region in the (Γ_0, Γ) plane. Another region was obtained by plotting the experimental value of Γ_0/Γ , taken from branching ratio measurements. The intersection of the two regions yields the values of Γ_0 and Γ . This is illustrated in Fig. 2 for the 8360 keV level obtained using the measured values of R and Γ_0/Γ and assuming $g=1.0$. The values of the Doppler widths Δ of the nuclear levels were deduced using $T_e=304$ K (at $T=300$ K) and obtained from Lamb's Theory¹⁰ with a Debye temperature $\theta_D=157$ K taken from specific heat data.¹⁹

Because of the dependence of the deduced values of $g\Gamma_0$ on the Doppler width and hence on T_e (see Sec. I), we tested the consistency of the above calculated value of T_e by measuring the temperature variation of the scattered cross section as discussed in Sec. III E.

Table III lists the values of $g\Gamma_0$ for nine levels as obtained from the averages of the three self-absorption measurements. The results for the remaining levels were derived from the present scattering values as discussed above. It may be noted that the self-absorption result of the 4432 keV level was corrected for the combined effects owing to the feeding from higher levels, and scattering from the unresolved ^{12}C level at 4439 keV. Furthermore, the three levels at 8826, 9213, and 9626 keV are unbound, the (γ, p) threshold being at 8793 keV. Their widths were determined by assuming the particle width $\Gamma_p=0$ (Table III).

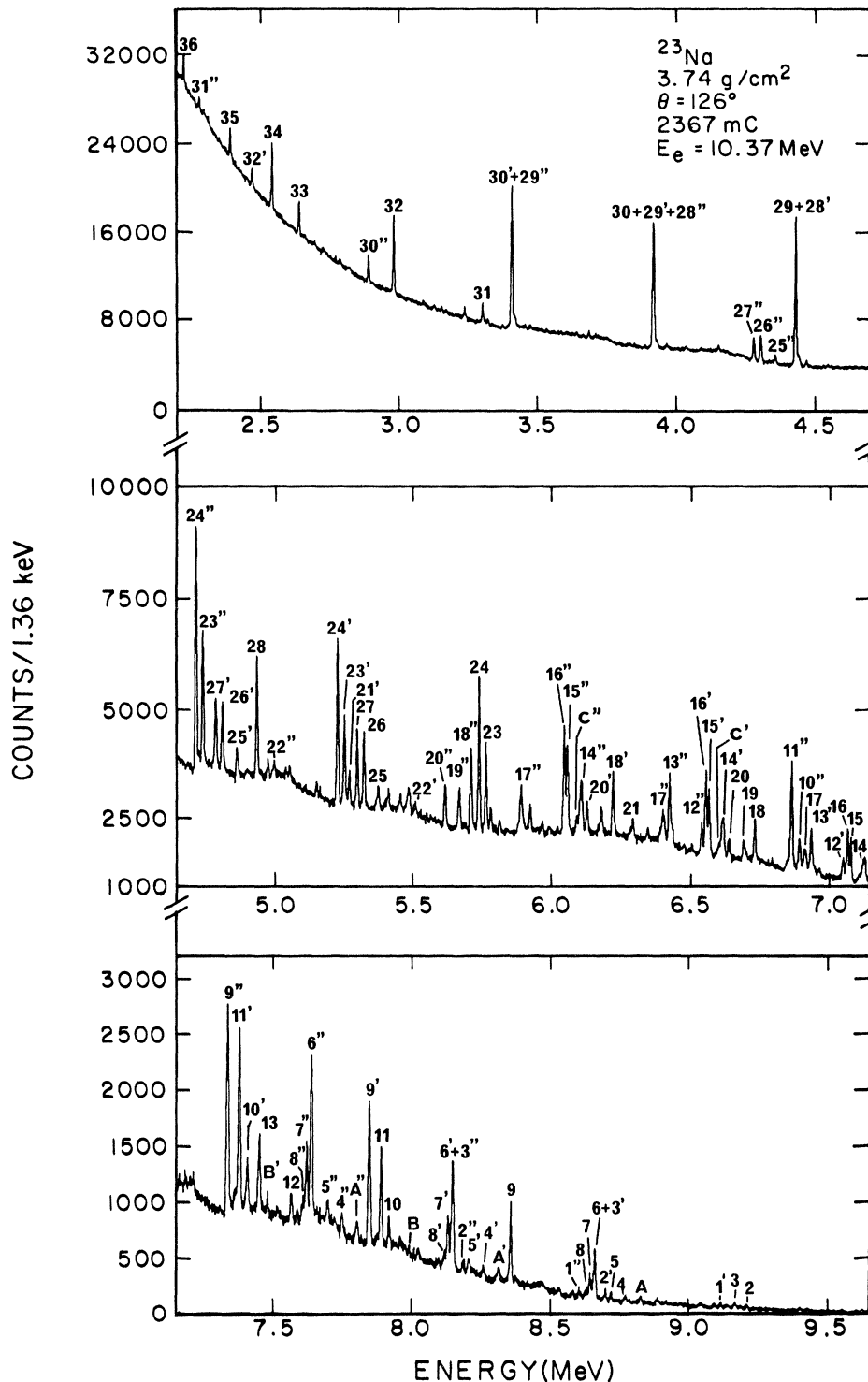


FIG. 1. Spectrum of scattered photons from a metallic Na target with 10.37 MeV bremsstrahlung. This is a sum of six spectra, obtained after passing the incident beam through a resonant Na absorber and a nonresonant Mg absorber. The single and double primes denote the single and double escape peaks, respectively. Each channel equals 1.36 keV. The list of γ -line energies corrected for nuclear recoil are given in Table I. Other symbols are explained in the text.

E. Temperature variation of scattered intensities

As mentioned in Secs. I and II, the scattered intensities from metallic ^{23}Na were measured at $T=298$ K and 78 K

after passing the beam through a 7.46 g/cm 2 thick resonant absorber of metallic Na at $T=298$ K (room temperature). The use of a resonant absorber in this measurement served to enhance the dependence of the scattered in-

TABLE I. Excitation energies in ^{23}Na obtained after correcting the γ line energies of Fig. 1 for recoil effects. Asterisks denote inelastic transitions where the corresponding initial and final states are indicated. Some weakly excited levels are labeled A, B, and C.

Peak No.	E_x (keV)	Transition	Peak No.	E_x (keV)	Transition
1	9626±3		18	6735±2.0	
2	9213±3		19	6694±2.0*	7134→440
3	9168		20	6642±2.0*	7082→440
A	8826±2		21	6295±2.0*	6735→440
4	8773±3*	9213→440	22	6022±2.0*	8662→2640
5	8721±2		23	5766±1.5	
6	8662±2		24	5741±1.5	
7	8645±2		25	5378±1.5	
8	8630±3		26	5326±1.5*	5766→440
9	8360±2		27	5301±1.5*	5741→440
10	7920±2*	8360→440	28	4938±1.5*	5378→440
B	7992±3				
11	7890±2		29	4432±1.5	
12	7566±2		30	3915±1.0	
13	7450±2*	7890→440	31	3302±1.0*	5378→2076
14	7134±3		32	2982±1.0	
	7117(^{16}O)		33	2640±1.0	
C	7122±3		34	2542±1.0*	2982→440
15	7082±2		35	2390±1.0	
16	7070±2		36	2223 $^1\text{H}(n,\gamma)^2\text{H}$	
17	6917(^{16}O)				

tensities on the Doppler widths of the ^{23}Na levels and hence on the T_e of metallic Na. The Lamb procedure for calculating T_e of Na yields $T_e=304$ K and $T_e=93$ K at $T=300$ K and $T=78$ K, respectively. Table IV compares the measured and predicted ratios $N(78\text{ K})/N(300\text{ K})$ of the scattered intensities using the above values of T_e . The good agreement obtained between the two sets of ratios shows the adequacy of the Lamb procedure¹⁰ for calculating T_e in the case of metallic Na. It should be remarked that the $g\Gamma_0$ values of the strongly excited levels of ^{23}Na as determined from the scattering cross section measure-

ments (being almost independent of T_e for thin scatterers) were very close to those obtained by self-absorption. This is a further confirmation of the above values of T_e .

It should be noted that in earlier works,^{12,20} similar temperature variation measurements were carried out on ^{62}Ni , ^{208}Pb , ^{15}N , and ^{11}B using elemental targets. The results indicated that while the Lamb procedure was successful²⁰ in predicting the scattering intensities versus T for ^{62}Ni and ^{208}Pb , it failed to do so in the cases of ^{11}B and ^{15}N . For ^{11}B , it was necessary to take into account the lattice binding properties of the boron atom¹² in the

TABLE II. Branching ratios (in %) of ^{23}Na levels from initial states E_x to final states E_f . The spins and parities J^π of the final states are indicated. The adopted values of the ground-state branching ratios are based on averaging the results of the present measurement with those reported in the literature (Ref. 17).

E_x (keV)	E_f (keV; J^π)						
	Adopted $0; \frac{3}{2}^+$	$0; \frac{3}{2}^+$	$440; \frac{5}{2}^+$	$2076; \frac{7}{2}^+$	Present work $2391; \frac{1}{2}^+$	$2640; \frac{1}{2}^-$	$3915; \frac{5}{2}^+$
5378	13±1	14±1	66±6	20±1			
5741	68±4	70±3	30±3				
5766	60±5	53±5	41±4		6±1		
6735	60±4	68±4	24±3		7±1		
7070	83±6	92±3					8±1
7082	56±2	55±2	25±4			20±2	
7890	63±4	58±4	36±3	6±1			
8360	71±3	71±3	20±1		9±2		
8662	87±3	91±4				9±1	

TABLE III. Measured widths of ^{23}Na levels obtained, in some cases, using scattering measurements, and in other cases, using self-absorption.

E_x^a (keV)	Γ_0/Γ (%)	$g\Gamma_0$ (eV)		J^π	
		This work	Others		
2982	58 ± 1^b	0.10 ± 0.02^d	0.05 ± 0.02^e	0.08 ± 0.02^b	$\frac{3}{2}^+$
3915	82 ± 2^b	0.06 ± 0.01^d		0.05 ± 0.01^b	$\frac{5}{2}^+$
4432	94 ± 2^b	0.95 ± 0.10^k	1.25 ± 0.20^e	1.07 ± 0.05^f	$\frac{1}{2}^+$
5378	13 ± 1^b	0.62 ± 0.09^d	0.40 ± 0.09^e	0.32 ± 0.06^g	$\frac{5}{2}^+$
5741	68 ± 4^b	1.18 ± 0.08	0.93 ± 0.18^e	0.84 ± 0.15	$(\frac{3}{2}, \frac{5}{2})^+$
5766	60 ± 5^b	0.78 ± 0.10	0.53 ± 0.10^e	0.58 ± 0.14^g	$(\frac{1}{2}, \frac{5}{2})^+$
6735	60 ± 4^c	0.66 ± 0.08	0.38 ± 0.08^e		$(\frac{3}{2}, \frac{5}{2})^+$
7070	83 ± 7^b	0.87 ± 0.09	0.75 ± 0.13^e	1.02 ± 0.21^h	$(\frac{3}{2}, \frac{5}{2})^+$
7082	56 ± 2^c	0.99 ± 0.12	0.85 ± 0.18^e	1.10 ± 0.22^h	$\frac{3}{2}^-$
7122	$(100)^b$	0.08 ± 0.03^d			
7134	37 ± 7^b	0.86 ± 0.20^d	0.95 ± 0.18^e	0.86 ± 0.17^h	$\frac{5}{2}^+$
7566	30 ± 20^b	0.77 ± 0.52^d	0.18 ± 0.05^e		
7890	63 ± 4^c	2.17 ± 0.22	2.75 ± 0.50^e		$\frac{5}{2}^+, T = \frac{3}{2}$
7992	$(100)^b$	0.07 ± 0.03^d			
8360	71 ± 3^c	2.15 ± 0.26	3.00 ± 0.50^e		$(\frac{3}{2}, \frac{5}{2})^+$
8630	$(100)^b$	0.11 ± 0.03^d			
8645	100^b	0.43 ± 0.05^d	0.78 ± 0.15^e		
8662	87 ± 3^c	1.41 ± 0.23	1.63 ± 0.27^e		$\frac{1}{2}^+, T = \frac{3}{2}$
8721	$(100)^b$	0.15 ± 0.02^d			
8826 ⁱ	36 ± 10^i	0.39 ± 0.14^i			$\frac{1}{2}^+$
9213 ^j	(100)	0.11 ± 0.04^j			
9626 ^j	$(100)^j$	0.10 ± 0.03^j			

^aThis work. Values of $g\Gamma_0$ are from self-absorption unless otherwise indicated.

^bResults taken from Ref. 17.

^cTaken from the adopted values of Table II.

^dScattering results combined with values of Γ_0/Γ . The errors include the uncertainty in the flux calibration.

^eScattering results taken from Ref. 6 (only statistical errors were reported).

^fReference 9.

^gReference 7.

^hReference 8.

ⁱThis level is unbound, hence the listed values are those of Γ_0/Γ_γ and $g\Gamma_0/\Gamma_\gamma/\Gamma$ instead of Γ_0/Γ and $g\Gamma_0$.

^jThe $g\Gamma_0$ of this unbound level was deduced by assuming that $\Gamma_p = 0$ and $\Gamma_0/\Gamma = 1$.

^kThis is an average over the scattering and the corrected self-absorption results (see the text).

particular target in order to get a consistent value of the effective temperature of ^{11}B . For ^{15}N , it was necessary to account for the contribution to T_e of the zero-point energy of vibration of ^{15}N in the diatomic $^{15}\text{N}_2$ molecule¹³ to get a correct value of T_e .

IV. DISCUSSION

The NRF process is selective in that only levels with large ground state widths Γ_0 and branching ratios Γ_0/Γ , and hence large Γ_0^2/Γ are expected to be strongly photoexcited. Thus the NRF technique is best suited for observ-

ing levels related to the ground state by $E1$ or $M1$ absorption. Since the ^{23}Na ground state is $\frac{3}{2}^+$, most of the excited levels should have $J^\pi = \frac{1}{2}^\pm, \frac{3}{2}^\pm$, and $\frac{5}{2}^\pm$ and few excited levels can have $\frac{7}{2}^+$ corresponding to pure $E2$ absorption. This is owing to the smaller probability of photoexciting higher multipoles, which, for the case of $M2$ transitions becomes negligibly small. This may be seen by noting that the single particle width of $M2$ transitions at 7 MeV, expressed in Weisskopf units (W.u.), is ~ 2 meV and the smallest Γ_0 that could be observed within the accuracy of the present measurements is ~ 30 meV. Further, any

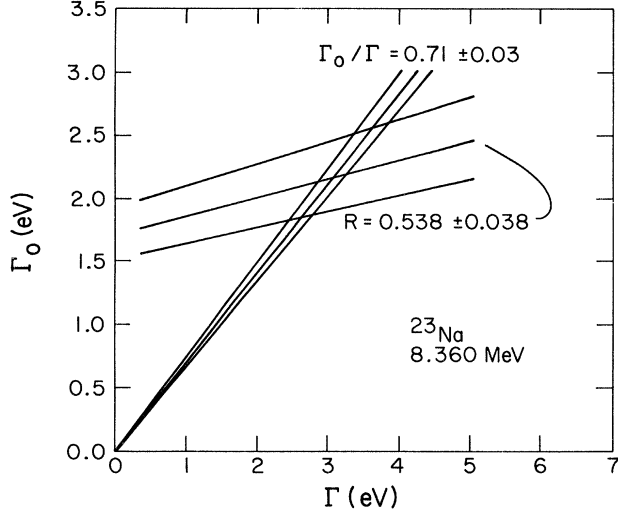


FIG. 2. Plot of the ground state branching ratio Γ_0/Γ and the nuclear self-absorption ratio in the (Γ_0, Γ) plane for the 8360 keV level in ^{23}Na . The intersection region defines the values of the Γ_0 and Γ together with the error bars.

width larger than 1 W.u. should, according to the compiled Nuclear Data results,²¹ be excluded as owing to a $M2$ transition. Similar arguments show that the probability of observing $E2$ transitions is not small and in fact a large number of such transitions were already observed in a recent NRF study²² of ^{40}Ca , with a higher atomic number, $Z=20$, which makes it more difficult for weak transitions to be observed.

The ^{23}Na nucleus contains 7 nucleons outside the ^{16}O core which are expected to be in the $2s-1d$ shell. Furthermore, most of the ^{23}Na levels below ~ 7 MeV are expected to involve neutron and proton excitations within the $2s-1d$ shells, hence, mostly $M1$ transitions should be excited. These expectations are in line with observations because among the 22 levels whose $g\Gamma_0$ were measured in the present work, 13 levels are known to have one of the following J^π values: $J^\pi = \frac{1}{2}^+$, $\frac{3}{2}^+$, and $\frac{5}{2}^+$ and, hence, obtained by $M1$ excitation. Only two levels at 7082 keV ($J^\pi = \frac{3}{2}^-$) and 9213 keV ($J^\pi = \frac{3}{2}^-$) were excited by $E1$ absorption which would involve either the excitation of the ^{16}O core or the promotion of one of the outer nucleons in ^{23}Na to an odd- l orbit such as $1f_{7/2}$ or $2p_{3/2}$. In addition, among the known $\frac{7}{2}^+$ levels, none were photoexcited in the present experiment. In the following, we discuss some levels in detail.

A. The 7070-keV and 8360-keV levels

These levels are reported to have one of the following J^π values: $J^\pi = \frac{3}{2}^+$, $\frac{5}{2}^+$, and $\frac{7}{2}^+$. The possibility of $\frac{7}{2}^+$ would imply pure $E2$ excitation and is very unlikely to occur as shown below. The strongest compiled $E2$ transition²¹ is known to reach 100 W.u. However, such strengths seem to decrease quickly with increasing transition energy. The strongest compiled ground state $E2$

TABLE IV. Calculated and measured ratios R_T of scattered intensities from metallic ^{23}Na targets at $T=300$ K and $T=78$ K.

E_x (keV)	R_T	
	Measured	Calc ^a
4432	0.70±0.07	0.68
5741	0.71±0.06	0.72
5766	0.76±0.08	0.79
6735	0.76±0.10	0.87
7070		
+7082	0.93±0.12	0.84
7890	0.75±0.08	0.78
8360	0.86±0.09	0.82
8662	0.95±0.12	0.89

^aThis calculation was carried out for a 3.61 g/cm² metallic Na target with a 7.46 g/cm² metallic Na absorber. The effective temperatures used were $T_e=304$ K at $T=300$ K and $T_e=93$ K at $T=78$ K and were deduced using the Lamb formula with $\theta_D=157$ K.

strengths with $E_\gamma > 7$ MeV is around 1 W.u., while an assignment of $J^\pi = \frac{7}{2}^+$ for the above two levels would require them to have a strength of 7.7 and 8.2 W.u., respectively, and would exclude a $\frac{7}{2}^+$ assignment. It should also be added that a $\frac{7}{2}^+$ assignment for the 7070-keV level may also be excluded because of Swann's observation⁸ that the 7070-keV level decay via 8% branch to the 2394 keV, $J^\pi = \frac{1}{2}^+$ level, implying an intense $M3$ transition strength (10^4 W.u.) which is very unlikely to occur. Further, a $\frac{5}{2}^+$ assignment for the 7070 keV level would also be difficult to understand because if the $E2/M1$ mixing amplitude, $\delta=1.6\pm 0.3$ (reported by Swann⁸) is correct, it would imply a very strong $E2$ transition of 7.4 W.u. From the above it would seem that the 8360 keV level is very likely to be either $\frac{3}{2}^+$ or $\frac{5}{2}^+$ while the 7070 keV level is $\frac{3}{2}^+$ with a small probability of being $\frac{5}{2}^+$.

B. The unbound levels

Three unbound levels occur at 8826, 9213, and 9626 keV. The first level is unbound by 33 keV and hence can not emit protons because of the Coulomb barrier. The other two levels were not observed by the $^{22}\text{Ne}(p,\gamma)^{23}\text{Na}$ reaction. However, it is important to note that the 9210 keV level reported in Refs. 17 and 23 and observed via the (p,γ) reaction should be different from that at 9213 keV found in the present work. If one assumes that these two levels are identical, then the measured quantities $\Gamma_0/\Gamma=0.7\%$ and $(2J+1)\Gamma_p\Gamma_\gamma/\Gamma=0.11\pm 0.3$ eV reported by Meyer,²³ together with our measured value $g\Gamma_0^2/\Gamma=0.11\pm 0.04$ eV, would imply $\Gamma_0=16$ eV, $\Gamma_p=0.03$ eV, and $\Gamma_\gamma=2240$ eV and, hence, would be impossible to occur. Here, it was assumed that $g=1$, but any other value would not change the above conclusion.

C. The $M1$ transitions, $T = \frac{1}{2}$

As noted above, most of the photoexcited levels in ^{23}Na are expected to decay to the $\frac{3}{2}^+$ ground state of ^{23}Na

TABLE V. Measured and predicted $B(M1\uparrow)$ values for the $T = \frac{1}{2}$ levels in ^{23}Na below 9 MeV. The last two levels have $T = \frac{3}{2}$. Asterisks indicate levels taken from Ref. 17 and not observed in the present work.

E_i (keV)	Experiment J^π	$B(M1\uparrow)$ (μ_0^2)	E_i (keV)	Predicted (Ref. 24) J^π	$B(M1\uparrow)$ (μ_0^2)
440*	$\frac{5}{2}^+$	0.616±0.034	411	$\frac{5}{2}^+$	0.607
2391*	$\frac{1}{2}^+$	0.002±0.0004	2323	$\frac{1}{2}^+$	0.059
2982	$\frac{3}{2}^+$	0.323±0.064	2747	$\frac{3}{2}^+$	0.461
3915	$\frac{5}{2}^+$	0.081±0.013 ^b	3893	$\frac{5}{2}^+$	0.098
4432	$\frac{1}{2}^+$	0.931±0.093	4311	$\frac{1}{2}^+$	1.143
5378	$\frac{5}{2}^+$	0.340±0.049	5246	$\frac{5}{2}^+$	0.253
5741	$(\frac{3}{2}, \frac{5}{2})^+$	0.532±0.036	5574	$\frac{5}{2}^+$	0.425
5766	$(\frac{1}{2} - \frac{5}{2})^+$	0.347±0.044	5745	$\frac{3}{2}^+$	0.280
6306*	$\frac{1}{2}^+$	a	5975	$\frac{1}{2}^+$	0.006
6735	$(\frac{3}{2}, \frac{5}{2})^+$	0.184±0.022	6493	$\frac{3}{2}^+$	0.326
6866*	$\frac{3}{2}^+, \frac{5}{2}^+$	a	6747	$\frac{5}{2}^+$	0.007
6946*	$(\frac{1}{2} - \frac{5}{2})^+$	a	6831	$\frac{3}{2}^+$	0.007
7070	$(\frac{3}{2}, \frac{5}{2})^+$	0.078±0.008 ^b	6836	$\frac{5}{2}^+$	0.001
7122		0.019±0.007	6945	$\frac{5}{2}^+$	0.354
7134	$\frac{5}{2}^+$	0.202±0.047	7906	$\frac{3}{2}^+$	0.014
7448*	$\frac{5}{2}^+$	a	7909	$\frac{5}{2}^+$	0.077
7566		0.152±0.102	8087	$\frac{5}{2}^+$	0.144
7720*	$\frac{1}{2} - \frac{5}{2}^+$	a	8092	$\frac{1}{2}^+$	0.036
7992		0.012±0.005	8167	$\frac{3}{2}^+$	0.012
8360	$(\frac{3}{2}, \frac{5}{2})^+$	0.314±0.038	8254	$\frac{1}{2}^+$	0.035
8469*	$(\frac{3}{2}, \frac{5}{2})^+$	a	8610	$\frac{5}{2}^+$	0.082
8630		0.015±0.004	8945	$\frac{3}{2}^+$	0.006
8645		0.057±0.006			
8721		0.019±0.002			
8826	$\frac{1}{2}^+$	0.048±0.017			
$\Sigma(T = \frac{1}{2})$		4.308±0.186	$\Sigma(T = \frac{1}{2})$		4.433
7890	$\frac{5}{2}^+, T = \frac{3}{2}$	0.377±0.038	7924	$\frac{5}{2}^+, T = \frac{3}{2}$	0.325
8662	$\frac{1}{2}^+, T = \frac{3}{2}$	0.185±0.030	8915	$\frac{1}{2}^+, T = \frac{3}{2}$	0.336

^aIn deducing the measured total $M1$ strength, the $B(M1\uparrow)$ value for this level was assumed to be $0.006 \mu_0^2$. With such a $B(M1\uparrow)$ value which corresponds to $g\Gamma_0^2/\Gamma = 30$ meV at 7.5 MeV, the level could have been easily missed within the detection limit of the present work (see the text).

^bThe $B(M1\uparrow)$ value was extracted after correcting $g\Gamma_0$ for the effect of the $E2/M1$ mixing amplitude (Refs. 8 and 17).

via $M1$ radiation. It is of interest to compare the findings of the present work with the large-scale shell-model calculations of Wildenthal^{5,24} in the sd shell region. In those calculations, one considers all the seven nucleons (three neutrons and four protons) outside the ^{16}O core in a complete basis space consisting of $1d_{5/2}$, $2s_{1/2}$, and $1d_{3/2}$ orbits. The Hamiltonian, consisting of two-particle matrix elements, was obtained by iteration to best fit 200 experi-

mental level energies in $A = 18-24$ nuclei. The single-particle energies were taken from ^{17}O . The wave functions thus obtained were used to predict the energy levels, particle-transfer strengths, electromagnetic moments, and transition rates between various levels in ^{23}Na .

Table V gives a comparison between measured and predicted values of the $M1$ strength. It is most convenient to compare the values of $B(M1\uparrow)$ because it can be ex-

pressed in terms of the measured quantity $g\Gamma_0$

$$B(M1\uparrow) = 0.448g\Gamma_{0i}/\Gamma_W = 85.3g\Gamma_{0i}/E_i^3,$$

where the Weisskopf unit Γ_W is defined as $\Gamma_W = 0.021E_i^3$. In this manner, one avoids the knowledge of the level spins. By definition we have also $(2J_0+1)B(M1\uparrow) = (2J_i+1)B(M1\downarrow)$.

In comparing the predicted and measured results in Table V, the $M1$ contribution of all levels known to have $J^\pi = \frac{1}{2}^+, \frac{3}{2}^+,$ and $\frac{5}{2}^+$ are included, some of which were taken from Ref. 17. It was assumed that all transitions are of pure dipole character except for cases for which the $E2/M1$ mixing amplitude δ is known.¹⁷ Furthermore, all other levels that were photoexcited in the present work except for the known odd-parity levels were assumed to be excited by pure $M1$ radiation. In this comparison, we focus our attention first to the $T = \frac{1}{2}$ levels because most of those levels were photoexcited in the present work. In Table V, a detailed comparison is presented only for the six lowest excited states with $J^\pi = \frac{1}{2}^+, \frac{3}{2}^+,$ and $\frac{5}{2}^+$. The agreement with the predicted values of Wildenthal²⁴ is remarkable for both the level energies and for the $B(M1\uparrow)$ values. For the higher-energy levels, it is impossible to make any detailed comparison because the spins of only a few levels are known with certainty and also because the ordering of the levels is not expected to be correctly predicted. Nevertheless, by combining the levels observed in the present work together with other $\frac{1}{2}^+, \frac{3}{2}^+,$ and $\frac{5}{2}^+$ levels reported in Ref. 17, one obtains a total of 25 levels below 9 MeV to be compared with 22 levels predicted by Wildenthal.²⁴ This is also an interesting agreement in view of the uncertainties involved in the J^π assignments of the levels and in their energies.

Another interesting result which may be obtained from Table V is the total $M1$ strength for the $T = \frac{1}{2}$ levels: The total measured $B(M1\uparrow)$ below 9 MeV is $4.31 \mu_0^2$ to be compared with a predicted value of $4.43 \mu_0^2$. This is considered to be an excellent agreement in view of all uncertainties involved. It should be pointed out that the $B(M1\uparrow)$ strength of all other predicted $T = \frac{1}{2}$ levels above 9 MeV (not given in Table V) is small, their combined strength is $< 3\%$ of the total $M1$ strength. Therefore, practically, almost all relatively strong $M1$ states with

$T = \frac{1}{2}$ were detected in the present work.

A few remarks should be added concerning Table V. The actual experimental $M1\uparrow$ strength could be larger than the above value, because our estimate was based on the assumption that $\Gamma_0/\Gamma = 1$ for some levels for which no experimental data were available. Obviously, this assumption underestimates the value of Γ_0 and hence of $B(M1\uparrow)$ because the scattering cross section is proportional to $g\Gamma_0^2/\Gamma$. This low estimate was probably more than compensated by the assumption that the levels of unknown parity are deexcited to the ground state via pure $M1$ radiation and that the $E2$ mixing amplitude was neglected for all cases where no data were available. Furthermore, because of counting rate and background considerations, all levels above 6 MeV (denoted by an asterisk in Table V) with small Γ_0/Γ such that $g\Gamma_0^2/\Gamma \leq 0.03$ eV are expected to be missed within the detection limit of the present experiment.

D. The $M1$ transitions, $T = \frac{3}{2}$

Most of the $T = \frac{3}{2}$ levels lie above the particle emission threshold and hence are unlikely to be excited using the present technique. Only two levels at 7890 keV ($J^\pi = \frac{5}{2}^+$) and 8662 keV ($J^\pi = \frac{1}{2}^+$) known¹⁷ to be $T = \frac{3}{2}$ (Table III) were photoexcited in the present work. The predicted excitation energies and $B(M1\uparrow)$ values are compared to the measured values in Table V. The total measured $B(M1\uparrow)$ is smaller by 15% than the predicted values in Table V. About 15 other $T = \frac{3}{2}$ levels up to 14 MeV excitation were predicted²⁴ (not listed in Table V) with a total $B(M1\uparrow)$ strength of $1.85 \mu_0^2$. In the present work, only about 30% of this $M1$ strength is observed. The remaining 70% $M1$ strength ($T = \frac{3}{2}$) should reside in the higher excited levels above the particle emission threshold.

ACKNOWLEDGMENTS

One of us (R.M.) would like to thank Prof. B. H. Wildenthal for some illuminating remarks and for sending his predicted results of ²³Na. This research was supported in part by the National Science Foundation under Grant NSF PHY 80-23603.

*Present address: Bell Laboratories, Holmdel, NJ 07733.

†Present address: Ben-Gurion University of the Negev, Beer Sheva, Israel.

‡Present address: Physics Department, University of Pennsylvania, Philadelphia, PA 19104.

¹J. Dubois, Nucl. Phys. **A104**, 657, (1967).

²M. Guttormsen, T. Pedersen, J. Reksad, T. Engeland, E. Osnes, and F. Ingebretsen, Nucl. Phys. **A338**, 141 (1980).

³S. G. Nilsson, K. Dan. Vidensk. Selsk. Mat.-Fys. Medd. **29**, No. 16 (1955).

⁴G. Alaga, K. Alder, A. Bohr, and B. R. Mottelson, K. Dan. Vidensk. Selsk. Mat.-Fys. Medd. **29**, No. 9 (1955).

⁵J. B. McGrory and B. H. Wildenthal, Annu. Rev. Nucl. Part.

Sci. **30**, 383 (1980).

⁶N. Shikazono and Y. Kawarasaki, Nucl. Phys. **A188**, 461 (1972).

⁷D. L. Friesel *et al.*, Phys. Rev. C **6**, 846 (1972).

⁸C. P. Swann, Nucl. Phys. **A167**, 201 (1971).

⁹F. R. Metzger, Phys. Rev. **136**, B374 (1964).

¹⁰W. E. Lamb, Phys. Rev. **55**, 190 (1939).

¹¹F. R. Metzger, Prog. Nucl. Phys. **1**, 53 (1959).

¹²R. Moreh, W. C. Sellyey, and R. Vodhanel, Phys. Rev. C **22**, 1820 (1980).

¹³R. Moreh, O. Shahal, and V. Volterra, Nucl. Phys. **A262**, 221 (1976).

¹⁴P. Axel *et al.*, Nucl. Sci. **NS22**, 1176 (1975).

- ¹⁵T. Chapuran, R. Vodhanel, and M. K. Brussel, Phys. Rev. C 22, 1420 (1980).
- ¹⁶D. F. Coope, L. E. Cannell, and M. K. Brussel, Phys. Rev. C 15, 1977 (1977).
- ¹⁷P. M. Endt and C. Van der Leun, Nucl. Phys. A310, 1 (1978).
- ¹⁸L. E. Cannell, Ph.D. thesis, University of Illinois, 1976.
- ¹⁹K. A. Gschneider, *Solid State Physics*, edited by F. Seitz and D. Turnbull (Academic, New York, 1964), Vol. 16, p. 368.
- ²⁰R. Moreh, O. Shahal, and I. Jacob, Nucl. Phys. A228, 77 (1974).
- ²¹P. M. Endt, At. Data Nucl. Data Tables 23, 3 (1979).
- ²²R. Moreh, W. M. Sandefur, W. C. Sellyey, D. C. Sutton, and R. Vodhanel, Phys. Rev. C 25, 1824 (1982).
- ²³M. A. Meyer and J. J. A. Smit, Nucl. Phys. A205, 197 (1973).
- ²⁴B. H. Wildenthal, Prog. Particle Nucl. Phys. (in press); (private communication).